International Journal of Thermophysics, Vol. 11, No. 1, 1990

Crystallization and Fibril Formation in Polymers[1]

E. J. Clark[2] and J. D. Hoffman[3]

Solutions of crystallizable polymers subjected to orientation crystallize in a fibrillar morphology if the polymer is solidified rapidly. The central core of the polymer fibers consists of thin, extended chain crystallites interspersed with disordered regions. The extended chain crystals are small fibrils having diameters generally less than a few hundred angstroms, while the lengths are usually not more than 5000 Å. These dimensions are limited by an unknown mechanism, because even in a saturated solution, the fibril crystal size is limited. Hoffman's theory of flow-induced crystallization predicts that cumulative strain limits the growth of the central core fibril such that the diameter and length of the fibril are an inverse function of undercooling. This study was undertaken to obtain data to test the theory. The dependence of the fibril dimensions on undercooling at the time of orientation has been studied. Polyethylene fibrils were made by shearing a dilute solution between two slides under isothermal conditions at an elevated temperature, and the dimensions of the resulting fibrils were measured with transmission electron microscopy. The fibril diameter appeared to be a function of undercooling, while the fibril length was constant and not a function of undercooling.

KEY WORDS: crystallization; fibrils; flow-induced; orientation-induced; polymers; polyethylene; undercooling.

1. INTRODUCTION

A fibrillar morphology results from crystallization of polymer solutions or melts subjected to elongational flow [1, 2]. Alignment of polymer molecules produces fibrillar crystals which influence the microstructure of

[1] Paper presented at the Tenth Symposium on Thermophysical Properties, June 20–23, 1988, Gaithersburg, Maryland, U.S.A.

[2] Thermophysics Division, National Institute of Standards and Technology (formerly National Bureau of Standards), Gaithersburg, Maryland 20899, U.S.A.

[3] Michigan Molecular Institute, Midland, Michigan 48640, U.S.A.

0195-928X/90/0100-0225$06.00/0

840/11/1-15

the solid polymer and enhance the physical and mechanical properties of polymer products. Thus, understanding factors which influence fibrillar morphology is important, especially since most polymer processes, e.g., fiber spinning, extrusion, mixing, blow molding, etc., involve flow processes which elongate polymer molecules.

The fibrillar morphology, shown in Fig. 1, consists of thin central fibril cores with regularly spaced overgrowths [3]. The elementary fibril core contains extended chain crystallites with lateral dimensions of a few hundred angstroms or less [4]. The overgrowths have polymer molecules intimately connected to the central core. The overgrowth lateral dimension is somewhat larger than the overgrowth spacing. The dimensions of polymer fibrils vary, but the length and diameter of the core fibril are limited by an unknown mechanism [3, 5]. Although the solution is saturated, the polymer fibril does not grow to an unlimited size.

Kinetic crystallization theories for polymers [2, 6] do not explain the dimensional limits of the fibrillar morphology. However, one theory for flow-induced crystallization predicts that cumulative strain limits growth of

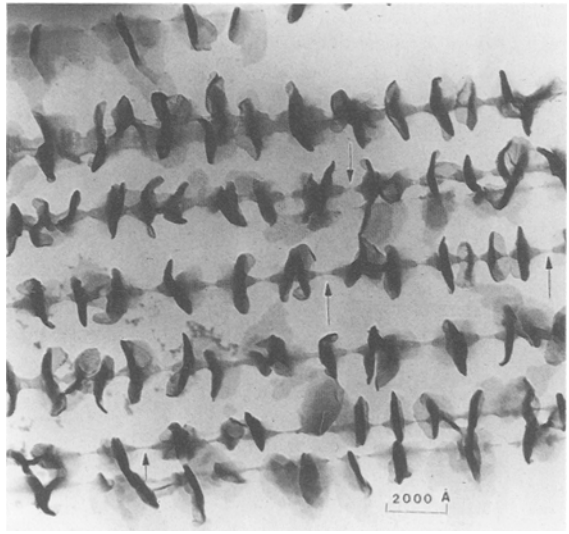

Fig. 1. Example of the regular appearance of shish kebabs made at 110°C from a 0.9% solution of polyethylene in octadecane. The shish kebabs were made by orienting the polymer solution between two slides by moving the top slide at a relative velocity of 10 cm · min^{-1} with respect to the lower slide. Arrows indicate core fibrils which appear stretched.

the central core fibril [5, 7]. This theory predicts the fibril diameter and length are inversely related to the undercooling.

$$D \approx \frac{C_1}{\Delta T}, \qquad L \approx \frac{C_2}{\Delta T}$$

where D is the diameter of the central core fibril, L is the mean characteristic length between overgrowths, C_1 and C_2 are constants which incorporate surface energy and material constants, and ΔT is the undercooling.

To test the theory, experiments were performed to determine the relationship between fibril dimensions and undercooling. Polymer fibrils were made under controlled flow conditions at four undercoolings. The diameter and length of the central core fibrils were measured to correlate the dimensions with undercooling and the results were compared with theory.

2. BACKGROUND

Polymers crystallize into two crystalline morphologies which grow according to two basically different processes [1–3], depending on whether the polymer is subjected to orientation or not. From unperturbed solutions or melts, polymers crystallize in a chain-folded morphology where the growth front proceeds perpendicular to the chain direction. The chain-folded crystal is platelet-like, with a thickness of 50 to 200 Å [8, 9]. The initial thickness is kinetically determined during nucleation and remains basically unchanged during crystallization [6]. By comparison, the remaining two dimensions grow very large during crystallization. Kinetic theories exist to explain the nucleation and growth process and the nature of the limited thickness of the chain-folded platelet [6].

Many methods of polymer orientation [2, 3] produce the fibrillar polymer morphology. The fibrillar morphology occurs in both solutions and melts and is relatively independent of the type of orientation and growth process. The limited dimensions of the fibrillar crystal recur for all preparations. In fibrous crystals, the polymer chains are oriented along the fiber axis in the flow direction [10], and growth is parallel to the chain direction [11, 12]. The fibril central core is composed of extended chain crystallites interspersed with shorter disordered regions, with the overgrowths anchored firmly in the backbone. Polymer fibrils with a thin central core and regularly spaced overgrowths are called "shish kebabs," with the central core the "shish" and the overgrowth the "kebab."

Two requirements necessary for fibrillar crystallization are a high molecular weight polymer and a process to elongate the polymer molecules

before crystallization. The importance of extensional flow in nucleation has been established. Other factors, such as temperature, molecular weight distribution, solution concentration, and elongation type and rate, also affect fibrillar crystallization.

Measurement of the fibril dimensions requires highly specialized instrumentation and special sample preparation, making it impossible to observe the elementary fibril formation during orientation experiments. The diameter of the elementary core fibril is generally reported between 50 and 300 Å [4, 11, 13], while the reported fibril lengths range from 250 to 2500 Å [4, 10, 11, 13–15]. The length values reported seem to be more dependent on the measurement method used.

Study of the fibrillar morphology naturally led to development of theories on nucleation and growth of orientation induced crystals [11, 15, 16]. George and Tucker [13] and Hoffman [5, 7] have proposed that overgrowths are nucleated at specific sites along the core fibril and that platelet spacing provides information about structural singularities in the backbone. Hoffman developed a theory for flow-induced crystallization accounting for the limited core fibril length and diameter. In this theory, the core fibril is considered to originate with multiple nucleation events on a flow-elongated molecule, resulting in an embryonic fibril that is a set of bundle-like nuclei. Repulsion of quasirandom coil chains in amorphous zones between nuclei builds up at the bundle ends as nuclei mature, leading ultimately to a high-end surface free energy and to volume strain in crystallites comprising the core fibril. This causes the diameter and length of the crystallites to be limited in a thermodynamic sense. The dependence of the diameter and length are calculated in terms of the driving force of crystallization. The fibril diameter and characteristic fibril length are predicted to depend on undercooling. The mean value of the core fibril diameter is

$$D = \left(\frac{0.7746}{\alpha^{1/2}} - \frac{1}{3}\right) \frac{6\sigma T_d^\circ}{(\Delta h_f)(\Delta T)} \tag{1}$$

where

σ = lateral surface free energy

α = volume strain parameter

T_d° = dissolution temperature

Δh_f = heat of fusion

T_{cr} = crystallization temperature

$\Delta T = T_d^\circ - T_{cr}$

This can be written

$$D = \frac{C_1}{\Delta T} \tag{2}$$

where

$$C_1 = \left(\frac{0.7746}{\alpha^{1/2}} - \frac{1}{3}\right)\frac{6\sigma T_d^\circ}{(\Delta h_f)} \tag{3}$$

The stable value of the mean characteristic fibril length is

$$L = \left(\frac{0.7746}{\alpha^{1/2}} - \frac{1}{3}\right)\frac{6\sigma_{eo} T_d^\circ}{(\Delta h_f)(\Delta T)} \tag{4}$$

where σ_{eo} = end surface free energy.

This can be written as

$$L = \frac{C_2}{\Delta T} \tag{5}$$

where

$$C_2 = \left(\frac{0.7746}{\alpha^{1/2}} - \frac{1}{3}\right)\frac{6\sigma_{eo} T_d^\circ}{(\Delta h_f)(\Delta T)} \tag{6}$$

The theory predicts that the basic core fibrils are quite thin at high undercoolings (ΔT large), but at lower undercoolings they have larger diameters. Since σ_{eo} is always greater than σ, the mean characteristic length is predicted to be considerable larger than the diameter.

3. EXPERIMENTAL

The fibrillar crystals were made by orienting a thin layer of dilute polyethylene mixture between two slides under isothermal conditions. The mixture was a 0.9% solution of Marlex 550[4] ($\bar{M}_w = 300{,}000$, $\bar{M}_n = 24{,}000$) polyethylene in octadecane. The crystals were examined in a transmission electron microscope (TEM), thus it was necessary to form them initially on a substrate suitable for the TEM. Special glass slides with carbon-coated mica surfaces were prepared to permit the thin carbon layer and crystals to

[4] Certain trade names are identified in order to specify adequately the experimental procedure. Such identification does not imply recommendation or endorsement by the National Institute of Standards and Technology.

be removed from the mica and transferred to a TEM sample holder. Dilute polyethylene solutions were used so the resulting shish kebabs would be spread out over the surface of the slide, permitting observation and measurement of individual shish kebabs.

The ovens were aluminum blocks with a small channel through the center of each. The ovens had resistance heaters on the exterior and were in balsa insulation to minimize thermal gradients. Their temperatures were stable and well controlled with temperature controllers which regulated to better than 0.01°C. The difference between the top and the bottom of the ovens was less than 0.04°C. Particular care was taken to assure that the shish kebabs were made under controlled orientation conditions at known temperatures.

The procedure for making the crystals was as follows. About 4 mg of a polyethylene–octadecane powder was weighed onto the carbon-coated surface of a slide and evenly distributed across the center area (about 2×1.5 cm). An identical carbon-coated slide was placed on top with the carbon face toward the polymer mixture. A small frame with a wire attached to one end was positioned around the top slide and then the slide sandwich and frame were placed into an oven at 155°C for about 4 min, during which time thermal equilibrium was reached. The oven temperatures were monitored using thermocouples embedded in the aluminum just below the center of each oven. When the temperature stabilized after the slide was inserted, it was judged that thermal equilibrium was attained. The slide sandwich was then carefully pushed to the center of a second oven set at the temperature desired for crystallization. When thermal equilibrium was reached (2 to 2.5 min) a motor was activated, which pulled the frame and top slide across the lower slide at a relative velocity of $10\ \text{cm} \cdot \text{min}^{-1}$ and out of the oven. This oriented the polymer solution between the slides and created the polymer fibrils. The top slide was immediately placed on cold mercury to quench the crystals and prevent rearrangement of the polyethylene. The lower slide was quickly removed from the oven and quenched similarly. Crystals were prepared at crystallization temperatures of 100, 105, 110, and 115°C.

The octadecane was removed by submerging the slide in room-temperature xylene. The slide was removed from the xylene and air-dried overnight. The crystals were prepared for the TEM by floating the carbon off the mica and onto 3-mm-diameter copper-mesh grids suitable for TEM examination. Twenty grids, arranged in a 4×5 matrix, were used to capture the carbon from each slide. Each grid was given a unique designation indicating location in the matrix.

The crystals were examined in a Phillips EM300 electron microscope operated at 80 kV in the transmission mode. Liquid nitrogen was kept in

the TEM cold trap at all times. On a daily basis, the microscope was adjusted for astigmatism and calibrated using magnification standards. Preliminary examination revealed many sizes of shish kebabs on all slides.

To produce a balanced data set for statistical analysis of the length and diameter measurements, a set of rules was devised to guide which grids and areas of the grids would be examined in the TEM. Criteria were also established for selection of the shish kebabs and the number of electron micrographs needed for statistical analysis. Two grids from the middle two rows of the center column of a grid were examined from the bottom slide. After initial scanning of the grid, two areas having the largest fibrils, based upon appearance of the length and diameter, were selected. In each area, the three largest fibrils with a minimum number of breaks or interruptions were photographed. Only fibrils not attached to neighboring fibrils and with at least four contiguous shish segments clearly visible from end to end were photographed. This resulted in 12 pictures at each of the four temperatures. Once a suitable shish kebab was identified on a picture, all segments with a clearly visible length and diameter were measured. The number of observations varied from picture to picture, and thus was not constant for all four temperatures.

The length of the largest shishes and the diameter of the associated kebabs were measured at the locations illustrated in Fig. 2. The fibril diameter (DC) was measured midway between adjacent kebabs, however, since it was not clear where the fibril ended, two measures of the fibril

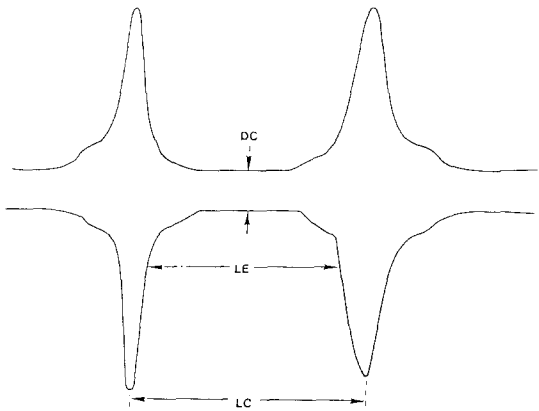

Fig. 2. Location of dimensional measurements made on each shish kebab. *DC* is the diameter of the fibril (shish) at the center. *LC* is the distance between the centers of two adjacent overgrowths (kebabs). *LE* is the fibril length between adjacent overgrowths.

length were made. The fibril length between the overgrowths (LE) was measured and the spacing between the centers of the overgrowths (LC) was measured. The length and diameter values reported were determined from dimensional measurements on enlarged prints of the electron image plates. The fibril dimensions were obtained by combining the magnification calibrations for each microscope setting with the measurements from the prints and the enlargement factor from the electron image plates.

4. DATA ANALYSIS

Nonclassical statistical techniques were used to analyze the data since the data did not have normal distributions and there was not an equal number of data observations at each temperature. Classical statistical techniques and tests assume a normal distribution of the measurements and/or constant variance [17, 18] and cannot be applied correctly if these assumptions are not met. When the data distribution is not normal, transformation of the data to a normal distribution is often necessary prior to use of standard statistical techniques [17]. The Box–Cox normality plot was used to determine if the data distribute normally and, if not, which transformation in the Box–Cox family yielded a transformed variable closest to being normally distributed. For analysis of variance (ANOVA), the BMDP Biomedical Computer Programs, P-Series [19], which do not assume an equal number of replicates per group to compute the variance among groups, were used to compute one-way ANOVA.

5. RESULTS AND ANALYSIS

The shish kebabs did not cover an entire grid; rather they occupied areas of varying size. The shish kebab orientation was always parallel with the direction of shear, and the shish kebab lengths ranged from just a few fibril sections to many microns. The general appearance of the shish kebabs was very regular along their length. The length of the fibril between kebabs was approximately the same for all shish kebabs on a grid, as can be seen in Fig. 1. However, a wide variation existed in the diameter size from one shish kebab to the next. Generally, on individual shish kebabs the fibril diameters were approximately uniform; however, when comparing the diameters among a group of shish kebabs, the diameters often differed by more than a factor of three. The shish kebab selection rules required selection of the largest shishes for the electron micrographs. The larger fibrils were selected to assure that fibrils examined were the more mature crystallites that had come closest to thermodynamic equilibrium. To deal with the data in this manner was clearly suggested by the nature of the three-

dimensional free energy–length–diameter diagram given in the theory [5, 7].

The median, mean, and standard deviation (SD) values of the diameter data for all temperatures are given in Table I, along with the coefficient of variation and the number of observations. The median and mean diameter values range from about 150 to 350 Å over the range of 100 to 115°C. The largest mean and median values occurred at 100°C, but the smallest diameters occurred at 105°C, with the values increasing between 105 and 115°C. Histograms of the data at each temperature and all temperatures together showed the data distribution to be nonsymmetric, with a tail of data points skewed toward the large diameters. A one-way ANOVA on the DC data grouping with respect to $1/\Delta T$ was done for the data from 105 to 115°C and showed an effect in $1/\Delta T$; however, the T test for the group means at the three undercoolings showed a 26% probability that the 110 and 115°C were not temperature dependent. A least-squares fit of the DC data across $1/\Delta T$ was done for the line $DC = C_1/\Delta T$. The slope, slope SD, and residual SD are listed in Table II. A plot of the residuals indicates some funneling as undercooling decreases.

Table I. Diameter and Length Measurements of the Largest Polyethylene Shish Kebabs[a] Observed

Variable	Temperature (°C)	Median value (Å)	Mean value (Å)	SD (Å)	Coefficient of variation	Number of observations
Diameter *DC*	115	235	249	62	0.25	112
	110	218	237	98	0.41	105
	105	148	155	50	0.32	90
	100	324	345	131	0.37	103
	All temperatures	227	250	112	0.45	410
Length *LE*	115	786	800	303	0.38	112
	110	856	854	321	0.38	105
	105	887	957	355	0.38	90
	100	877	897	247	0.28	103
	All temperatures	846	873	312	0.36	410
Length *LC*	115	943	986	362	0.37	112
	110	1090	1096	359	0.33	105
	105	1183	1253	445	0.36	90
	100	1191	1152	278	0.24	103
	All temperatures	1086	1115	374	0.34	410

[a] The shish kebabs were made from a 0.9% solution of Marlex 550 polyethylene in octadecane by orienting the solution between glass slides moving at a rate of 10 cm · min^{-1}.

Table II. Least-Squares Fit of Length and Diameter Data Variables

Variable[a]	Model	Temperature range (°C)	Intercept (Å)	Intercept SD	Slope Å · °C	Slope SD	Residual SD
DC	$\log(DC) = A + (B/\Delta T)$	105–115	4.46	0.92	15.50	1.63	0.336
LE	$(LE)^{1/2} = A + (B/\Delta T)$	100–115	32.24	0.98	−63.86	18.91	5.22
LC	$(LC)^{1/2} = A + (B/\Delta T)$	100–115	37.63	1.02	−94.81	19.77	5.46
DC	$DC = (C_1/\Delta T)$	105–115	—	—	3908	79	78
LE	$LE = (C_2/\Delta T)$	100–115	—	—	16077	397	416
LC	$LC = (C_2/\Delta T)$	100–115	—	—	20443	500	522

[a] Length and diameter values are in Å.

A Box–Cox normality plot of the diameter data indicated that the log function was the best power transform. The $\log(DC)$ data were plotted as a function of $1/\Delta T$, where $\Delta T = T_d^\circ - T_x$, with $T_d^\circ = 129.4°C$ [20], the polyethylene dissolution temperature in octadecane. Diameter measurements did not follow a single trend for all four temperatures. A one-way ANOVA on the $\log(DC)$ data grouping with respect to $1/\Delta T$ was also done from 105 to 115°C and demonstrated a clear effect on the $\log(DC)$ grouping in $1/\Delta T$. This effect was confirmed by a significantly nonzero slope in a least-squares fitted line, the line fit being done across groupings of $\log(DC)$ according to $1/\Delta T$. When $\log(DC)$ was plotted as a function of undercooling, a least-squares fitted line to the 105–115°C data showed $\log(DC) = 4.46 + 15.50/\Delta T$. The estimated values of the slope and intercept and their SDs are given in Table II, along with the residual SD. The residuals from this fit show negligible temperature dependence and the T test comparing the group means of the three data sets had only a 2% probability that the 110 and 115°C data are not temperature dependent. Thus, the $\log(DC)$ data had a clear dependence on undercooling between 105 and 115°C.

The diameter data from 100°C did not follow the same trend as the data for other temperatures. The mean value of the 100°C data was much larger than at any other temperature. The most likely explanation for this is that as a result of the large undercooling (30°C), the polyethylene had begun to crystallize before the solution orientation started. This is supported by the fact that single crystals were observed on the carbon substrate in a few electron micrographs.

The raw LE data range from around 250 to almost 2000 Å. The fibril length measurements between kebabs (LE) are tabulated in Table I for each temperature and for all the data combined. The median LE length values lie between 786 and 887 Å. Histograms of the LE data showed that the data did not have a normal distribution, but a tail going toward the high LE values. The fit of the line $LE = C_2/\Delta T$ with the data was poor. The slope, slope SD, and residual SD for this fit are listed in Table II. The residuals show a distinct temperature dependence.

A Box–Cox normality plot indicated that the square root was the best power function to transform the LE data to normality. The $(LE)^{1/2}$ data plotted versus $1/\Delta T$ showed a slight decline with increase in undercooling. The model fitted was $(LE)^{1/2} = A + B/\Delta T$. The estimated values of the slope and intercept and their SDs are given in Table II. A one-way ANOVA on the $(LE)^{1/2}$ data grouping with respect to $1/\Delta T$ was done using data for four temperatures and had a slope very near zero. The LE data are essentially constant at $10\ \text{cm} \cdot \text{min}^{-1}$ and are not a function of undercooling.

The mean and median LC length data are also tabulated in Table I.

These values are 25 to 30% higher than the corresponding LE values. Analysis of the data showed that the LC data follow the same trends as the LE data. The least-squares fits of the LE data and $(LE)^{1/2}$ data are shown in Table II for comparison. The LC data also show a very small effect in $1/\Delta T$ and appear to be essentially constant, not a function of undercooling.

The present work suggests that for flow-induced crystallization, Hoffman's theory predicts the correct general order of magnitude for the fibril diameter and the observed decrease in fibril diameter on increased undercooling. For fibril length, the theory gives a reasonable estimate of the order of magnitude, but the prediction of length as a function of undercooling is not supported by the data from this study. Currently it is believed that only a relatively minor modification of the theory is required to bring its predictions into accord with experiment. The modification involves a slightly different assumption concerning how the strain is distributed into the crystal proper at the crystal–amorphous interface at the ends of each "shish." Whatever be its failings in its present form regarding certain details, no other theory explains the order of magnitude of the fibril length and diameter, at the same time explaining why the core fibril fails to grow larger even in supersaturated solutions.

6. CONCLUSIONS

Flow-induced crystallization of dilute polyethylene solutions resulted in fibrillar crystals of a shish kebab morphology having overgrowths fairly regularly spaced on a central core fibril of limited dimensions. Wide distributions in the shish kebab sizes were found at each temperature.

The fibril diameter data showed a clear dependence on undercooling between 105 and 115°C. The best least-squares fit to the 105 to 115°C data for the center fibril diameter versus undercooling is $\log(DC) = 4.46 + 15.50/\Delta T$. The median diameter of the largest fibrils increased from 148 to 235 Å between 105 and 115°C. However, the diameters at 100°C were much larger than for other temperatures. It was concluded that this increase probably resulted from the nucleation of chain-folded polyethylene crystals prior to orientation.

The fibril lengths showed no dependence on crystallization temperature, being essentially constant for all four temperatures. The median value of fibril length ranged from 786 to 887 Å as measured from the visible ends of the core fibril, excluding the kebab thickness. The overgrowth spacing measured between the centers of adjacent kebabs was about 25 to 30% longer.

Hoffman's theory of flow-induced crystallization predicts the correct general order of magnitude of the fibril diameter and length, and it

properly predicts the diameter decrease as the undercooling increases. However, the theory predicts the fibril length is a function of undercooling, whereas the data from this study indicate that the fibril length is constant when the flow rate is constant.

ACKNOWLEDGMENT

The Authors acknowledge Dr. Freddy Khoury of the National Institute of Standards and Technology for providing the electron microscopy facilities and necessary guidance.

REFERENCES

1. A. J. Pennings, *J. Cryst. Growth* **48**:574 (1980).
2. A. Keller, *J. Polym. Sci. Polym. Symp.* **59**:1 (1977).
3. A. J. McHugh, *Polym. Eng. Sci.* **22**:15 (1982).
4. A. Zwijnenburg, P. F. van Hutten, A. J. Pennings, and H. D. Chanzy, *Colloid Polym. Sci.* **256**:729 (1979).
5. J. D. Hoffman, *J. Res. Natl. Bur. Stand. (U.S.)* **84**:359 (1979).
6. J. D. Hoffman, in *Treatise in Solid State Chemistry, Vol. 3*, N. B. Hannay, ed. (Plenum Press, New York, 1976), pp. 497–615.
7. J. D. Hoffman, *Polymer* **20**:1071 (1979).
8. F. Khoury and E. Passaglia, in *Treatise in Solid State Chemistry, Vol. 3*, N. B. Hannay, ed. (Plenum Press, New York, 1976), pp. 335–496.
9. D. C. Bassett, *Principles of Polymer Morphology* (Cambridge University Press, New York, 1981).
10. A. J. Pennings and A. M. Kiel, *Kolloid Z. Z. Polym.* **205**:160 (1965).
11. A. J. Pennings, J. M. A. A. van der Mark, and A. M. Kiel, *Kolloid Z. Z. Polym.* **237**:336 (1970).
12. A. J. Pennings, C. J. H. Schouteten, and A. M. Kiel, *J. Polym. Sci. Part C* **38**:167 (1973).
13. W. George and P. Tucker, *Polym. Eng. Sci.* **15**:451 (1975).
14. P. F. van Hutten and A. J. Pennings, *Makromol. Chem. Rapid Commun.* **1**:477 (1980).
15. D. T. Grubb and M. J. Hill, *J. Cryst. Growth* **48**:321 (1980).
16. A. Keller and M. J. Machin, *J. Macromol. Sci. Phys.* **B1**:41 (1967).
17. P. F. Velleman and D. C. Hoaglin, *Applications, Basics, and Computing of Exploratory Data Analysis* (Duxbury Press, Boston, 1981).
18. G. W. Snedecor and W. G. Cochran, *Statistical Methods*, 6th ed. (Iowa University State Press, Ames, 1967).
19. W. J. Dixon and M. B. Brown, eds., *BMDP-79: Biomedical Computer Programs P-Series.* (University of California Press, Los Angeles, 1979).
20. T. W. Huseby and H. E. Bair, *J. Appl. Phys.* **39**:4969 (1968).